

THIN FILMS ON LINAC BEAMS AS NON-DESTRUCTIVE DEVICES FOR  
PARTICLE BEAM INTENSITY, PROFILE, CENTERING AND ENERGY MONITORS

L. Wartski

Institut d'Electronique Fondamentale, Laboratoire associé au CNRS  
Université de Paris-XI, Bâtiment 220-91405 Orsay (France)  
and

S. Roland, J. Lasalle, M. Boloré and G. Filippi  
Département de Physique Nucléaire, CEN-Saclay  
B.P. 2-91190 Gif-sur-Yvette (France)

Summary

The optical transition radiation emitted by electron irradiated aluminum, silver, gold-coated plates and self-supported metallic and mylar films has been investigated experimentally using 45° incident electron beams with intensities from 100 pA up to 10 μA, and energies from 35 up to 72 MeV. Beam diagnostics (intensity, profile, centering, energy) were made using an appropriate optical arrangement together with a two-parallel foils device in which the interference phenomena in transition radiation emitted at both interfaces was exploited.

The intensity of light integrated in a small aperture at the center of the interference pattern presents a strong particle-energy dependence (of the form  $\sim E^8$ ) which was used in the optimization of the phase adjustment of the electron bunches in the linac at small current intensities. Moreover, study of the visibility of fringes yields to an estimate of the transverse momentum spread of the electron beam and to the r.m.s. angle of multiple scattering in a given material.

Introduction

It is now well established that, when a uniformly moving charged particle crosses an interface separating two media with different optical properties, it emits the so-called transition radiation, a specific effect which was predicted more than 25 years ago by Frank and Ginzburg<sup>1</sup> after the discovery of the Cerenkov effect. Actually, this radiation can be considered as a Cerenkov effect of the second order and is produced, more generally, whenever a charged particle passes through an electrically inhomogeneous medium<sup>2</sup>.

In recent years, this effect was studied both theoretically and experimentally, mainly in the X-ray region of the spectrum; the application to the detection and identification of individual particles was the main goal of scientists concerned with nuclear physics, high energy physics instrumentation, cosmic rays or astrophysics.

This paper reports results of measurements of the effect in the optical region of the spectrum for electron beams instead of individual particles interacting with matter and outlines the application of transition radiation to particle diagnostics.

-----  
This work was supported by the Commissariat à l'Energie Atomique C.E.N. Saclay (France).

Theoretical background

Single interface

If a single particle of charge  $e$  and normalized energy  $\gamma$  crosses an interface from the medium to the vacuum, the intensity of the transition radiation emitted into the vacuum (forward emission) in a frequency range  $d\omega$  and a solid angle  $d\Omega$  is given by

$$\frac{d^2 W}{d\omega d\Omega} = \frac{e^2}{\eta^2 c} \cdot \frac{\alpha^2}{(\alpha^2 + \gamma^{-2})^2} \quad (1)$$

where  $\alpha$  is the angle of emission with respect to the charge velocity.

This simple formula was derived from the more general expression given by Garibyan<sup>3</sup> for the normal incidence and is only valid for ultra relativistic particles and in the case where the complex dielectric constant of the medium is such that  $|\epsilon| > 1$ .

The radiation is of the dipole type and is consequently linearly polarized, the electric vector lying in the plane containing the normal to the interface and the direction of emission. The intensity maximum occurs in a direction making an angle  $\alpha_M = \gamma^{-1}$  with respect to the normal to the interface. It should be noted that, under the above mentioned conditions, the intensity of radiation given by equation (1) does not depend on the angle of incidence of the electron nor on the optical properties of the traversed medium.

When the particle crosses the interface from the vacuum to the medium, the intensity of the transition radiation into the vacuum ("backward" emission) is obtained by multiplying formula (1) by a Fresnel term  $F(\Psi, \alpha, \omega)$  for reflection and corresponding to the actual angle  $\Psi$  of incidence of the particle;  $\alpha$  is now the angle of the emission with respect to the direction of specular reflection. This property can be understood using the pseudo-photon formalism (Williams-Weizsäcker method).

Two parallel interfaces at a distance L

In this case (figure 1) the front face of the second foil plays the role of a mirror for the forward radiation produced by the first foil. The radiation field adds in phase with the backward radiation of the mirror since both are produced by the same traversing electron. The resulting interference pattern is centered around the direction of specular reflection. The phase difference between the two sources of radiation in any direction making an

angle  $\alpha$  with the direction of specular reflection is given by

$$\phi = \frac{2\pi L}{\lambda\beta} (1 - \beta \cos \alpha) \quad (2)$$

where  $L$  is the length of the electron path between the foils and  $\beta$  the electron velocity expressed in units of  $c$ .

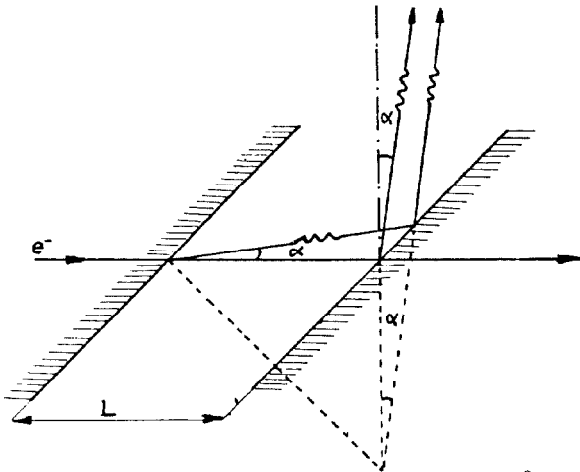


Figure 1 : Two parallel foils ( $\psi = 45^\circ$ ) metal - vacuum and vacuum - metal case.

Formula (2) is easily derived by considering two sources localized on the foils and oscillating with a phase difference related to the time of flight of the electron from one foil to the other.

In this case, the intensity of transition radiation is given by equation (3).

$$\frac{d^2W}{d\omega d\Omega} = \frac{4e^2}{\pi^2 c} \cdot F(\psi, \alpha, \omega) \frac{\alpha^2}{(\gamma^{-2} + \alpha^2)^2} \sin^2 \left[ \frac{\pi L}{2\lambda} (\gamma^{-2} + \alpha^2) \right]$$

Owing to the high directivity of radiation in the case of ultra relativistic electrons, the Fresnel term can be considered as  $\alpha$  independent.

It should be noted that this interference phenomenon is analogous to the interference phenomena obtained in pure optical experiments by the "division of amplitude" technique in a plane parallel plate (transmission type interference). As it is well known, in such experiments, fringes localized at infinity (also often called fringes of equal inclination) are observed even in the case of extended sources of radiation<sup>4</sup> (in our case, the electron beam impinging on the foils extends across the transverse directions).

The interference order is given by

$$p = \frac{L}{2\lambda} (\gamma^{-2} + \alpha^2) \quad (4)$$

The angular radii of intensity maxima  $\alpha_M$  and minima  $\alpha_m$  are given by

$$\alpha_{M,m} = \left[ (p - p_0) \frac{2\lambda}{L} \right]^{1/2} \quad (5)$$

where  $p$  is an integer  $k$  for  $\alpha_m$  and  $p = k + 0.5$  for  $\alpha_M$ .

At the center of the pattern, the interference order is generally fractional and takes the form

$$p_0 = \frac{L}{2\lambda} \gamma^{-2} \quad (6)$$

### Experimental arrangement

The experimental work was performed on the Saclay 80 MeV electron linac.

The samples were prepared by vacuum deposition of aluminum, silver and gold on mylar foils  $3.5 \mu\text{m}$  thick. Thicknesses of the metal coatings were estimated to be about  $0.4 \mu\text{m}$  using a weighing procedure.

These samples were stretched over a ring using a drumhead tightening principle.

In the study of the properties of transition radiation, thicker substrates (quartz plate  $0.4 \text{ mm}$  thick) were used in place of the second traversed foil, in order to obtain better mirror properties.

"Bulk" materials of different thicknesses were also used, i.e. aluminum foils from  $0.75 \mu\text{m}$  up to  $15 \mu\text{m}$ , silver foils from  $0.5 \mu\text{m}$  up to  $3 \mu\text{m}$  and gold foils of  $0.1 \mu\text{m}$  thickness.

The thinner foils used, manufactured by Goodfellow Metals Limited, had a precision on thickness of 10% and a purity of 99.7%. Unlike the backed foils, they were glued on the ring holders. As these thin self-supported foils were always used in place of the first traversed foil giving thus the forward radiation, the poor flatness obtained by this technique was not considered as an important failure.

Moreover, unlike the backed foils, these self-supported foils could be irradiated by high current densities without suffering any damage.

The foils in which the "backward" radiation was produced were fastened to a rotating disc (figure 2) and were positioned in the path of the beam by remote control at an angle of incidence  $\psi = 45^\circ$ .

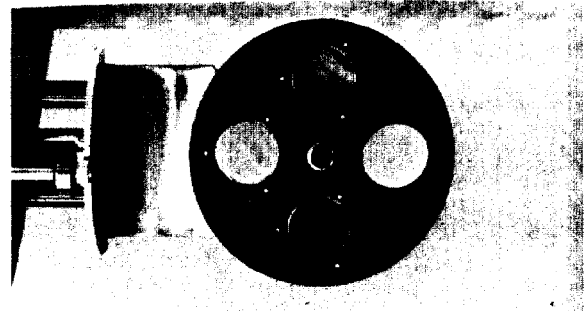


Figure 2: Rotating disc supporting the foils.

In the irradiation chamber was placed either one of these foils inclined at  $45^\circ$  to the beam direction or two parallel foils having the same inclination.

The elements of the optical arrangement have been described in some details in a previous paper<sup>5</sup>. We recall the principal features of this arrangement:

a) A scanning mirror is used in order to record the angular transition radiation patterns both in the incident plane of the samples (plane containing the electron trajectories and the normal to the samples) and in the plane perpendicular to the latter. This mirror and a multiturn potentiometer are driven by a stepping motor.

b) Radiation emitted at a given angle  $\alpha$  is formed by a lens into a ring of radius  $R = f \tan \alpha$  ( $f = 142\text{cm}$  is the focal distance of the lens) whatever the distance between the electron trajectory and the optical axis of the apparatus. A diaphragm of radius  $R$  positioned in the focal plane of this lens permits the registration of photons emitted in a given angular interval ( $0 - \alpha_0$ ). This arrangement is commonly used in gas Cerenkov counters and was set up in reference 6. The angular distribution can be studied either by the use of the scanning mirror (the light selected by a diaphragm being detected by a 56 DUVP photomultiplier), or by a direct photographic registration in the focal plane of the lens and microdensitometer analysis<sup>7</sup>.

c) The image of the irradiated foils is formed with a magnification equal to unity in a given plane and is recorded either with a TV camera or a photo-camera.

d) A system of two-crossed slits located in this image plane permits the registration of the beam profile.

e) A reference cross illuminated by a lamp is located in this image plane in order to achieve the precise beam positioning.

f) The selection of a given wavelength interval or the study of the transition radiation spectrum was made using either interference filters or a Ebert-Fastie-25cm monochromator.

g) All the optical elements were positioned along the line of sight of the accelerator using as a reference the light emitted by the cathode of the electron gun.

Mean-intensities of the accelerated electron beam were in the range  $100 \text{ pA} - 10 \mu\text{A}$ .

The energy of the beam could be varied from 35 up to 72 MeV.

The Energy of the beam was measured at the optimum RF phase adjustment by the deflecting magnet with a 1% resolution slit, and the energy variations were simply achieved by changing the phase of the RF field in the last accelerating section by means of a stepping motor.

As it was pointed out in reference<sup>8</sup>, this procedure avoids a number of problems including magnet hysteresis. The instrumentation used in the measurement of the  $\gamma$ -dependence of transition radiation is shown in figure 3. The fraction of transition radiation selected by the remotely controlled diaphragm is detected, after wavelength filtering, by the 2 ns. rise-time-high gain photomultiplier; the output-pulse voltage of the latter is displayed on the sampling scope which is manually adjusted to sample only at a time corresponding to the steady-state of the machine. This adjustment avoids transient beam-loading effects at high intensity currents.

The resulting integrated signal forms the Y-input of the X-Y recorder. The X-axis is driven by the analog output of the swept phase of the fourth klystron and represents relative beam energy with respect to the fixed maximum energy. During the measurement, the output of the toroidal current transformer is permanently controlled on a conventional scope.

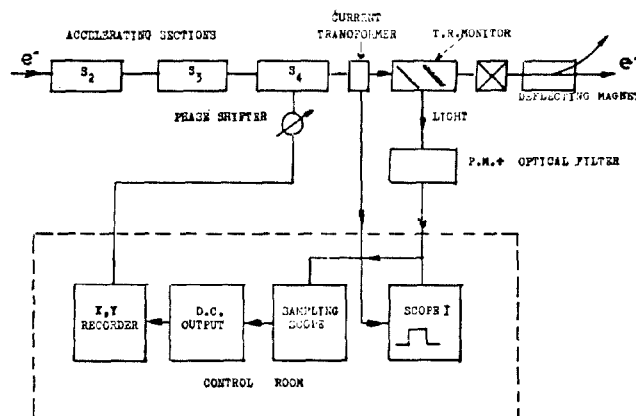


Figure 3 : Instrumentation used in the measurement of the  $\gamma$ -dependence of transition radiation.

## Results

Figure 4 shows the angular distribution of the "backward" transition radiation emitted by a single vacuum-aluminum interface inclined  $45^\circ$  to the beam direction when a good resolution is used and when the analyzing mirror is scanned in the plane containing the beam axis and the normal to the boundary.

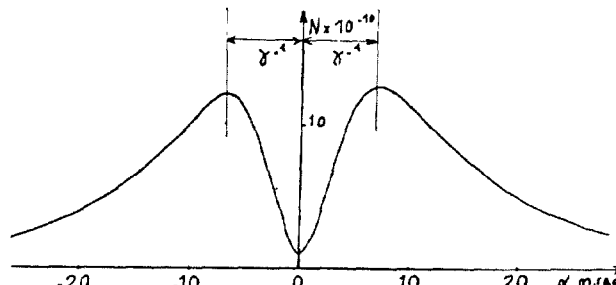


Figure 4: "Backward" radiation pattern  
 $N =$  number of photons/ electron/  $\Delta$   
 $\lambda = 4530 \text{ \AA}$  ;  $\gamma = 1.25$  ;  $\alpha_0 = 0.5 \text{ m rad}$ .

The angular distance of the maxima was measured on a number of similar patterns recorded at different values of  $\alpha_0$  and drawing chords for better accuracy in the determination of these maxima. The extrapolation at vanishingly small angles  $\alpha_0$  and the comparison of the obtained value of  $\gamma$  to the value given by the conventional momentum measurement lead to the conclusion that the energy could be measured by this technique with a precision better than 3%.

The experimental "backward" radiation yield in the investigated wavelength region (from 2500 up to 6000 Å) and for an aluminum boundary is shown on figure 5.

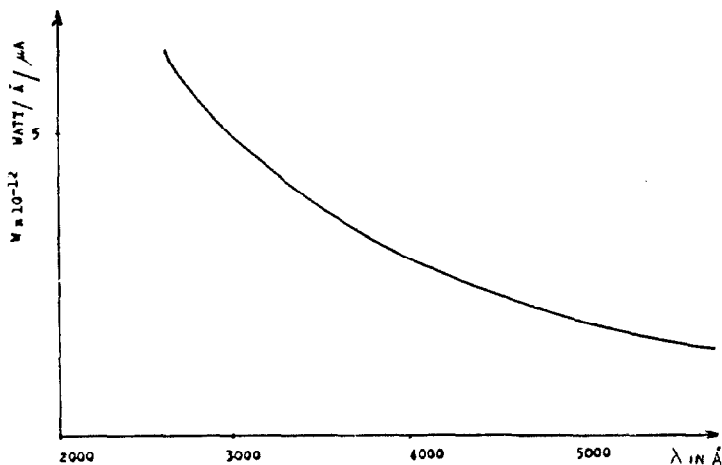


Figure 5 : Absolute " backward" radiation yield from an aluminum boundary  $\psi=45^\circ$ ;  $\gamma=125$

Here, the radiation was integrated in a cone with apex angle  $\alpha_0 = 3\gamma^{-1}$ . The shape of this spectrum demonstrate the general property of a  $\lambda^{-2}$  dependence. (We recall that, following Garibyan's theory, the forward emission spectrum extends in the X-ray region up to a cut-off frequency  $\omega_c = \gamma\omega_p$ , where  $\omega_p$  is the plasma frequency of the medium). This property agrees very well with the wavelength dependence predicted by transition radiation theory since the reflectance of aluminum in this wavelength range is practically constant ( $\approx 90\%$ ).

Integration over  $\lambda$  gives an overall radiation yield of about 10 nW per  $\mu A$  of incident electrons.

Another characteristic property of transition radiation which was emphasized in reference 9 and 5 is that the radiation yield increases but logarithmically with  $\gamma$  provided  $\alpha_0 \gamma \gg 1$ .

Figure 6a is the photographic image of the electron-irradiated foils and shows the actual size of the electron beam since the magnification was just equal to unity, as was above mentioned. The two foils arrangement was used here in order to avoid the registration of the cathode light, and the radiation was integrated over all angles of emission. Moreover, the beam profile was recorded using the two crossed slits (defining an aperture of  $1\text{mm}^2$ ) and photomultiplier detection. From this registration, the beam diameter was estimated to

about 3mm at half intensity.

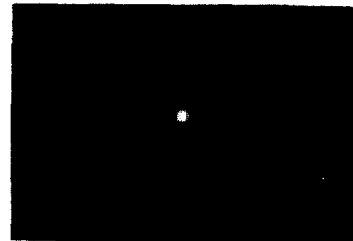


Figure 6a : Image of the electron-irradiated foils giving the actual size of the electron beam;  $\gamma=125$ ;  $I=13\text{mA}$ ; pulse width= $2\mu\text{s}$ ; frequency = 500 Hz; time exposure = 0.25 s; film sensitivity= 3000 Asa.

Figure 6b shows the image of the electron-irradiated foils displayed on the T.V. scope (55850 type vidicon tube) and the illuminated reference cross located in the image plane of the foils. This spot was still visible at a mean intensity of about 10nA.

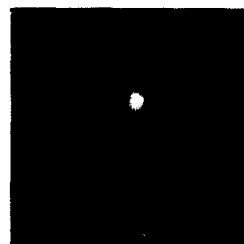


Figure 6b : Image of the electron-irradiated foils displayed on the T.V. scope. Two-foils arrangement ( $L=25.5\text{mm}$ );  $\gamma=125$ ;  $I=13\text{mA}$ ; pulse width =  $2\mu\text{s}$ ; frequency=500 Hz;

In order to check the possibilities of this system as a current-monitor at low intensities, a study was made using the electrons produced by field emission in the RF coupling device of the first accelerating section. These electrons are further accelerated and radiate when they cross the foils.

The output pulse voltage of the photomultiplier is shown on figure 7.

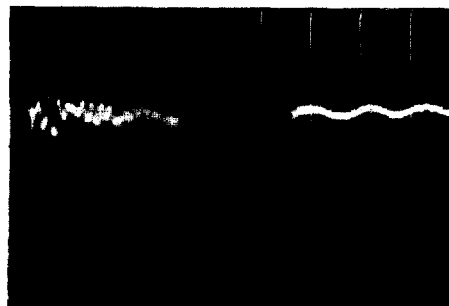


Figure 7 : Low- intensity current monitoring. (56 DUVP photomultiplier with 1800 V bias) horizontal: 500 ns/cm; vertical: 50 mV / cm.

The peak intensity of this field emission current was measured starting with higher intensity currents monitored by the toroidal

current transformer, and adjusting the attenuation factor of a set of optical attenuators in order to obtain the same output pulse voltage. This procedure gave a peak intensity of about 0.4  $\mu$ A. It was still possible to record the beam profile in this situation and the beam diameter was estimated to about 12 mm. at half intensity.

In the case of two-parallel foils arrangement in which the distance L is much greater than  $2\lambda\gamma^2$ , i.e. when the interference order at the center of the pattern is not too small, one can observe a substantial number of fringes of equal inclination. Figure 8 shows the photographic registration of the interference pattern in the case where  $p_0 = 0.76$ .



Figure 8 : Interference pattern obtained with the two-parallel foils arrangement  
 Foil 1: Aluminum-coated mylar 3.5  $\mu$ m thick  
 Foil 11: Aluminum-coated quartz 0.4  $\mu$ m thick  
 L : 13.5 mm;  $\psi$  : 45° ;  $\lambda$  : 4390 Å ;  $\Delta\lambda$  : 140 Å ;  $\gamma$  : 141.9  
 I : 13 mA; pulse width : 1.5  $\mu$ s; frequency : 62.5 Hz;  
 Time exposure : 2 min; polaroid film sensitivity : 3000 Asa.

The fringes could also be observed using the technique of the scanning mirror and photomultiplier detection of the light integrated in a small aperture of the diaphragm. In most of our applications, this versatile technique was preferred to the photographic registration which is more time-consuming.

The angular radii corresponding to the successive maxima  $\alpha_M$  and minima  $\alpha_m$  were measured and gave an excellent agreement with the theoretical values deduced from equation (

It was also observed that integration over a large angle gave a radiation yield which was, to within a few percents, twice the radiation yield given by a single foil.

On the other hand, the intensity of light at the center of the pattern, integrated in a given small aperture, has interesting properties related to its  $\gamma$ -dependence.

Figure 9 shows the evolution of this intensity versus  $\gamma$ . The maxima and minima cor-

respond respectively to constructive and destructive interference.

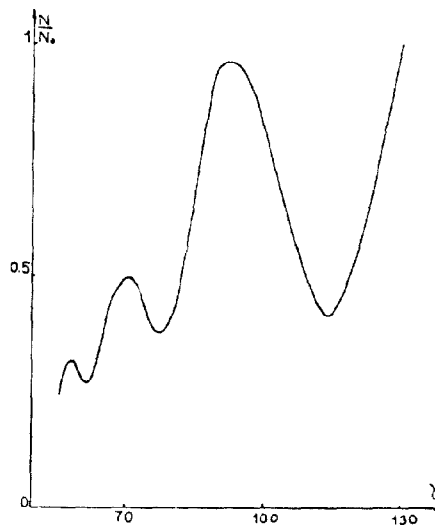


Figure 9:  $\gamma$ -dependence of the relative intensity of light at the center of the pattern for the two-foils arrangement.  
 L: 9.9 mm;  $\lambda$ : 4530 Å ;  $\Delta\lambda$ : 190 Å ;  $\alpha_0$  : 2.8 mrad.

The most remarkable behaviour of this registered pattern is the increased dependence of intensity on  $\gamma$ , as compared with the case of the single foil. From figure 9, it can be seen that, for certain ranges of  $\gamma$ , a variation of 1% in  $\gamma$  gives a corresponding variation of about 8% in the signal.

A straightforward application of this strong  $\gamma$ -dependence was the optimization of the phase adjustment of the electron bunches in the accelerating sections. For a 1  $\mu$ A accelerated mean current, this adjustment was achieved in the range  $\pm 2^\circ$  of the RF phase shifter.

The first minimum ( $p_0 = 1$ ) was extrapolated to vanishingly small apertures and the value of  $\gamma$  obtained was in excellent agreement with theory (theoretical value  $\gamma = 104.5$ ; experimental  $\gamma = 105.5$ ). It can then be suggested that a device using interference phenomena in transition radiation could be a simple tool for energy measurements with a precision of about 1%.

Figure 10 shows the manifestation of the strong  $\gamma$ -dependence on the output pulse voltage of the photomultiplier.

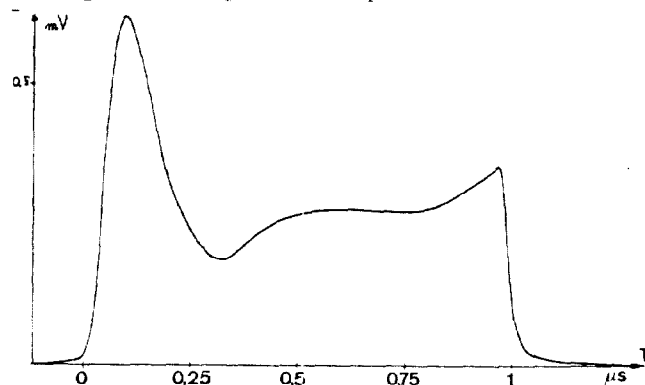


Figure 10: L: 9.9 mm;  $\lambda$ : 4530 Å ;  $\Delta\lambda$ : 190 Å ;  $\alpha_0$  : 2.8 mrad ; I : 130 mA

The rapid decrease after the rise-time is related to the transient beam loading effect.

The visibility of fringes is a function of  $\Delta\lambda$  and  $\Delta\gamma$  but also of  $\langle\alpha_b^2\rangle$  and  $\langle\alpha_s^2\rangle$  which account for the angular spread of the beam and the multiple scattering when it traverses the first foil. The former parameters were determined and injected into a computing program. The latter, which are more important, were determined by theory when a centered Gaussian distribution for the angle of the electrons emerging from the first foil was taken into account.

Experiments were made using successively different calibrated thicknesses for the first foil, using for instance a stack of one, two or three identical aluminum foils 0.75  $\mu\text{m}$  thick.

Resolving equation of the form

$$\langle\alpha_b^2\rangle + n\langle\alpha_s^2\rangle = \sigma^2, \text{ where } n \text{ is the}$$

number of piled-up foils and the  $\sigma$  r.m.s. angle in the Gaussian distribution giving the best fit between experiment and theory, yield the following values at  $\gamma=140$ :

$$\langle\alpha_b^2\rangle^{1/2} = 0.3 \text{ mrad and } \langle\alpha_s^2\rangle^{1/2} = 0.7 \text{ mrad}/\mu\text{m}$$

#### References

1. I. Frank and V. Ginzburg, J. Phys. USSR 9, 353 (1945).

2. F.G. Bass and V.M. Yakovenko, Theory of radiation from a charge passing through an electrically inhomogeneous medium, Sov. Phys. Usp. vol. 8, No. 3, 420 (1965).
3. G.M. Garibyan, Contribution to the theory of transition radiation, Sov. Phys. JETP, vol. 6, No. 6, 1079 (1958).
4. M. Born and E. Wolf, Principles of optics (Pergamon Press, New York, 1964); chapter 7.
5. L. Wartski, J. Marcou and S. Roland, Detection of optical transition radiation and its application to beam diagnostics, IEEE Trans. on Nuclear Science, vol. NS 20, No. 3, 544 (1973).
6. A.I. Al'khanyan, K.A. Ispiryan and A.G. Oganesyan, An experimental investigation of transition radiation and its possible application to measure the energies of fast particles, Sov. Phys. JETP, vol. 29, No. 6, 964 (1969).
7. D.K. Aitken, R.E. Jennings, A.S.L. Parsons and R.N.F. Walker, Transition radiation in Cerenkov detectors, Proceedings Phys. Soc., vol. 82, part. 5, No. 520, 710 (1963).
8. R.F. Koontz, G.A. Loew and R.H. Miller, Single bunch radiation loss studies at SLAC, IEEE Trans. on Nuclear Science, vol. NS 19, 491 (1971).
9. J. Oostens, S. Prunster, C.L. Wang and L.C.L. Yuan, Transition radiation from relativistic charged particles and its energy dependence, Phys. Rev. Letters, vol. 19, No. 9, 541 (1967).